Molecular BioSystems

PAPER

View Article Online
View Journal | View Issue

Published on 17 February 2016. Downloaded by Politechnika Warszawska on 25/04/2016 09:51:58.

Cite this: *Mol. BioSyst.*, 2016, 12, 1333

Phosphorylation of thymidylate synthase affects slow-binding inhibition by 5-fluoro-dUMP and N^4-hydroxy-dCMP

Jan Ludwiczak,†[a] Piotr Maj,†[a] Piotr Wilk,†‡[a] Tomasz Frączyk,§[a] Tomasz Ruman,[b] Borys Kierdaszuk,[c] Adam Jarmuła[a] and Wojciech Rode*[a]

Endogenous thymidylate synthases, isolated from tissues or cultured cells of the same specific origin, have been reported to show differing slow-binding inhibition patterns. These were reflected by biphasic or linear dependence of the inactivation rate on time and accompanied by differing inhibition parameters. Considering its importance for chemotherapeutic drug resistance, the possible effect of thymidylate synthase inhibition by post-translational modification was tested, *e.g.* phosphorylation, by comparing sensitivities to inhibition by two slow-binding inhibitors, 5-fluoro-dUMP and N^4-hydroxy-dCMP, of two fractions of purified recombinant mouse enzyme preparations, phosphorylated and non-phosphorylated, separated by metal oxide/hydroxide affinity chromatography on $Al(OH)_3$ beads. The modification, found to concern histidine residues and influence kinetic properties by lowering V_{max}, altered both the pattern of dependence of the inactivation rate on time from linear to biphasic, as well as slow-binding inhibition parameters, with each inhibitor studied. Being present on only one subunit of at least a great majority of phosphorylated enzyme molecules, it probably introduced dimer asymmetry, causing the altered time dependence of the inactivation rate pattern (biphasic with the phosphorylated enzyme) and resulting in asymmetric binding of each inhibitor studied. The latter is reflected by the ternary complexes, stable under denaturing conditions, formed by only the non-phosphorylated subunit of the phosphorylated enzyme with each of the two inhibitors and $N^{5,10}$-methylenetetrahydrofolate. Inhibition of the phosphorylated enzyme by N^4-hydroxy-dCMP was found to be strongly dependent on $[Mg^{2+}]$, cations demonstrated previously to also influence the activity of endogenous mouse TS isolated from tumour cells.

Received 12th January 2016,
Accepted 17th February 2016

DOI: 10.1039/c6mb00026f

www.rsc.org/molecularbiosystems

Introduction

Thymidylate synthase (TS; EC 2.1.1.45), a prominent target for fluoropyrimidines and antifolates in chemotherapy,[1–4] catalyzes 2′-deoxyuridine-5′-monophosphate (dUMP) C(5) methylation, producing 2′-deoxythymidine-5′-monophosphate (dTMP).[5] The enzyme potent inhibition by 5-fluoro-dUMP (FdUMP) is responsible for the antiproliferative activity of certain fluoropyrimidines, including 5-fluorouracil, 5-fluorodeoxyuridine (FdUrd), 5-fluorocytosine and trifluorothymidine prodrugs.[6–8] Several reports presented a possible mechanism of resistance to FdUrd based on alteration of the target enzyme causing less potent inhibition by FdUMP.[9–15] While several of those reports documented the ability of the enzyme's mutation(s), either naturally occurring[12,13] or experimentally induced,[11,14] to influence properties, in the case of parental and FdUrd-resistant mouse leukemia L1210 cells alteration of thymidylate synthase expressed by the resistant cells was found to involve posttranslational modification(s), rather than a mutation.[15] However, although phosphorylation appeared involved, such conclusions could not be documented unequivocally (ref. 15; *cf.* 16).

It should be mentioned that drug resistance limits effectiveness of chemotherapy, used to treat different pathogens, including infectious agents,[17–21] as well as cancer,[22,23] with tumours resistant to drugs, both intrinsically (present before treatment) and acquired as a result of treatment, being mostly caused by altered drug metabolism or drug target.[22,23]

Both FdUMP and N^4-hydroxy-dCMP (N^4-OH-dCMP) are competitive *vs.* dUMP, slow-binding and $N^{5,10}$-methylenetetrahydrofolate-dependent thymidylate synthase inhibitors,[24] causing

[a] *Nencki Institute of Experimental Biology, 3 Pasteur Street, 02-093 Warszawa, Poland. E-mail: rode@nencki.gov.pl; Fax: +48-22-822 5342; Tel: +48-608351155*
[b] *Department of Chemistry, Rzeszów University of Technology, 6 Powstańców Warszawy Ave., 35-959 Rzeszów, Poland*
[c] *Institute of Experimental Physics, Warsaw University, Warszawa, Poland*
† These authors contributed equally.
‡ Present address: Soft Matter and Functional Materials Macromolecular Crystallography (BESSY-MX), Elektronenspeicherring BESSY II, Albert-Einstein-Str. 15, D-12489 Berlin, Germany.
§ Present address: Institute of Biochemistry and Biophysics, Polish Academy of Sciences, 5a Pawińskiego Street, 02-106 Warszawa, Poland.

Published on 17 February 2016. Downloaded by Politechnika Warszawska on 25/04/2016 09:51:58.

time-dependent inactivation of the enzyme.[25] When studied with endogenous thymidylate synthases, isolated from tissues or cultured cells, the dependence of the inactivation rate on time was usually biphasic, the inactivation rate decreasing after about 2 min of enzyme preincubation with one of the inhibitors (ref. 24, 26–32; *cf.* 33). Biphasic FdUMP binding by human recombinant thymidylate synthase was also presented.[34] Thus differing interactions are suggested by the inhibitor with two binding sites on the enzyme molecule that may be interpreted in terms of negative cooperativity. In this context, it should be mentioned that although TS is a homodimer with two equivalent active sites, each composed of residues from both subunits, it shows half-the-site activity, with associated negative cooperativity,[35–37] the latter questioned recently to occur with the bacterial enzyme.[38] However, as presented in Table 1, the enzyme isolated from certain sources showed linear dependence of rate of inactivation by FdUMP on time, and both behaviors could be found in enzyme preparations isolated from sources of the same specific origin. Of particular interest is the group of mouse TSs (Table 1), as the coding sequences of both L1210 parental and FdUrd-resistant cell TSs proved to be identical to that of the mouse enzyme,[15] suggesting the observed differences, including those concerning inactivation parameters, result from posttranslational modification. Furthermore, the difference between inhibition profiles observed with L1210r and L1210r* enzyme preparations (Table 1) pointed to possible influence of phosphorylation.

In order to test a possibility of thymidylate synthase inhibition to be affected by post-translational modification, *e.g.* phosphorylation, two metal oxide/hydroxide affinity chromatography (MOAC)-separated fractions, phosphorylated and non-phosphorylated, of the recombinant mouse enzyme were compared with respect to sensitivity to inhibition by each of two slow-binding inhibitors, FdUMP and N^4-hydroxy-dCMP.

Table 1 Parameters for inactivation of thymidylate synthases from different mouse, rat and human sources by FdUMP. The plots of log (remaining activity) *vs.* time were either linear or biphasic (*cf.* ref. 24), the latter suggesting different interactions of each inhibitor with the two binding sites on the TS molecule. With the biphasic plots, inhibition constants and inactivation rate constants were calculated with the use of apparent inactivation rate constants during the initial (0.0–1.5 min) and later (4–10 min) periods of preincubation with a given inhibitor at various concentrations. The corresponding inhibition constants and inactivation rate constants are then K_i' and k_2' and K_i'' and k_2'', respectively

Enzyme source	Inactivation rate dependence on preincubation time	K_i' (nM)/k_2' (min^{-1})	K_i'' (nM)/k_2'' (min^{-1})
Mouse TS			
Thymus[a]	Biphasic[b]	2.6/0.24	61/0.44
L1210p[c]	Biphasic	1.8/0.17	20/0.12
L1210r[c]	Biphasic	12.2/0.25	14/0.06
L1210p*[d]	Biphasic	15.3/0.22	6.5/0.10
L1210r*[d]	Linear[e]	47.5/0.59	
Ehrlich carcinoma[f]	Biphasic	6/0.18	71/0.17
Rat TS			
Regenerating liver[c]	Biphasic	10/0.29	15/0.14
Colon tumour K-12[g]	Linear	120/1.2	
Human TS			
CCRF-CEM leukemia[f]	Biphasic	4/0.18	6/0.11
Colon tumour HCT-8[g]	Linear	130/0.8	

[a] Ref. 26. [b] The inactivation rate lowered after 2 min of preincubation of the enzyme with the inhibitor. [c] Ref. 24. [d] Ref. 15. [e] The inactivation rate did not change during the entire time of preincubation of the enzyme with the inhibitor. [f] Ref. 27. [g] Ref. 30. L1210p and L1210r are mouse leukemia L1210 cells parental and 5-FdUrd-resistant, respectively; the enzyme from L1210p* and L1210r* cells was purified in the presence of protein phosphatase inhibitors.

Experimental

Pro-Q® Diamond Phosphoprotein Gel Stain and SYPRO® Ruby Protein Gel Stain are from Molecular Probes.

Enzyme preparations

Cloning of the mTS coding region into the pPIGDM4+stop vector and its expression as a HisTag-free protein in thymidylate synthase-deficient TX61- (a kind gift from Dr W. S. Dallas) *E. coli* strain was previously described.[39]

Purification of the enzyme was done at 2–4 °C with 20 mM 2-mercaptoethanol and phosphatase inhibitors (50 mM NaF, 5 mM Na-pyrophosphate, 0.2 mM EGTA, 0.2 mM EDTA and 2 mM Na_3VO_4) present in all buffers. The cell pellet, collected following centrifugation of 1 l of *E. coli* culture, was suspended in 100 ml of 50 mM sodium/potassium phosphate buffer, pH 7.5, containing 0.1 M KCl, immersed in an ice-ethanol bath and sonicated (Branson Sonifier 250), applying ten pulses of 60 s each, separated with 15 s pauses. After removal of cell debris by centrifugation for 20 min at 20 000 × *g*, 2% streptomycin sulfate was added to the supernatant, the suspension stirred for 20 min and the precipitated nucleic acid was removed by 20 min of centrifugation at 20 000 × *g*. Solid ammonium sulfate was added to the stirred supernatant to 30% saturation and, after additional 20 min of stirring, the resulting mixture was centrifuged for 20 min at 20 000 × *g*. The ammonium sulfate content of the supernatant was raised to 80% saturation and, after stirring for 20 min, the resulting precipitate was spun down. It was dissolved in 10 mM sodium/potassium phosphate buffer, pH 7.5, dialyzed overnight against two 2 liter changes of the same buffer and loaded onto a DE-52 column (2.5 × 7 cm) equilibrated with the above buffer. The column was washed with 150 ml of the same buffer, followed by 250 ml of 25 mM sodium/potassium phosphate buffer pH 7.5, and the enzyme was eluted with 50 mM sodium/potassium phosphate buffer, pH 7.5. Fractions containing thymidylate synthase activity were pooled and precipitated with solid ammonium sulfate at 80% saturation. Following centrifugation, the pellet was dissolved in 10 mM sodium/potassium phosphate buffer, pH 7.5, containing 1 M ammonium sulfate, and loaded onto a phenyl-Sepharose column (1.5 × 7 cm) equilibrated in the same buffer. The column was washed with 200 ml of the same buffer and the enzyme was eluted with 10 mM sodium/potassium phosphate buffer, pH 7.5, containing 0.8 M ammonium sulfate. The most active and purest fractions (assessed electrophoretically) were pooled and

 This journal is © The Royal Society of Chemistry 2016

Published on 17 February 2016. Downloaded by Politechnika Warszawska on 25/04/2016 09:51:58.

concentrated in an Amicon Column Eluate Concentrator apparatus. TS activity was measured either spectrophotometrically[40] or with the use of the tritium release assay.[27] The final preparation was highly homogeneous, as judged by SDS/PAGE analysis of samples containing up to 40 μg protein. Its specific activity (the tritium release assay) was 1.75 μmol min^{-1} mg $protein^{-1}$ at 37 °C.

The purified TS preparation was separated into phosphorylated and non-phosphorylated fractions using MOAC on $Al(OH)_3$ beads (ref. 41; *cf.* 16).

Electrophoretic analysis and testing the presence of phosphate groups

Purified enzyme preparations were analyzed by polyacrylamide gel (7.5%) electrophoresis under non-denaturing conditions (4 °C, 150 V, 90 min, electrode buffer containing 25 mM Tris and 192 mM glycine), and by SDS/polyacrylamide gel (12.5%) electrophoresis according to Laemmli.[42] Following electrophoresis, gels were fixed by incubation in 50 mM Tris-HCl, pH 8.0, containing 25% (v/v) 2-propanol.[43] Then the assay for the presence of protein phosphate groups, with the use of the Pro-Q® Diamond Phosphoprotein Gel Stain, followed by staining of the same gel for protein by SYPRO® Ruby Protein Gel Stain was performed as previously described.[15]

Kinetic studies

Quantitative analyses of thymidylate synthase slow-binding inhibition by FdUMP and N^4-OH-dCMP, leading to time-dependent inactivation of the enzyme, were performed by following the decrease of enzyme activity with time (usually at 0.5, 1, 1.5, 4, 6, 8, and 10 min) during preincubation of the enzyme at 37 °C in the presence of 0.4 mM (6*RS*)-meTHF, 3.3 μM dUMP (to prevent thermal inactivation), and various concentrations of inhibitor. Activity remaining after preincubation was determined by addition of 50 μM [5-^{3}H]dUMP (4×10^4 dpm $nmol^{-1}$) and measurement of tritium release following 4 min incubation.[32] The slopes of the semi-log plots of percent remaining activity *vs.* preincubation time, expressing apparent inactivation rate constants (k_{app}) and corresponding inhibitor concentrations ([I]), were then replotted as double-reciprocal plots, and the values of k_2 and K_i were determined from the plot intercept and slope, respectively.[44]

Results and discussion

Comparative analysis of m-TS and m-pTS

TS preparation of mouse recombinant TS expressed in bacterial cells, highly purified in the presence of phosphatase inhibitors and analyzed with the Pro-Q® Diamond Phosphoprotein Gel Stain following SDS-PAGE, showed the presence of low levels of phosphorylated protein (not shown). Enrichment of the phosphorylated fraction, by separation from non-phosphorylated, using MOAC on $Al(OH)_3$ beads, yielded ≈1% of the total purified TS protein. Electrophoretic comparison of the non-phosphorylated with enriched phosphorylated fraction allowed for confirmation of the effective separation of m-pTS from m-TS and demonstrates

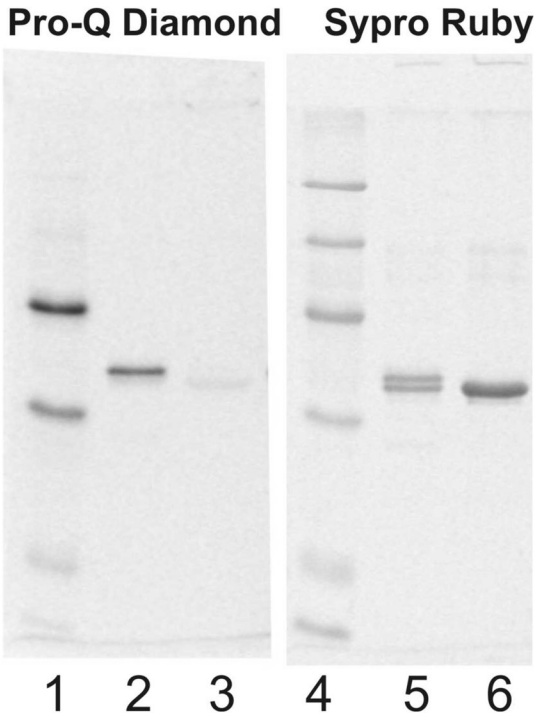

Fig. 1 Phosphorylated (lanes 2 and 5) and non-phosphorylated (lanes 3 and 6) fractions (separated by MOAC on $Al(OH)_3$) of recombinant mouse TS preparation, and PeppermintStick™ phosphoprotein molecular weight standards (lanes 1 and 4), analyzed for phosphoprotein/protein following SDS-PAGE. Gels were stained with Pro-Q® Diamond Phosphoprotein Gel Stain, to reveal phosphoprotein, followed by SYPRO Ruby Protein Gel Stain, in order to detect total protein (note: both fluorescent stains were applied on the same gel in a series, with the gel image collected following each staining, as instructed by the vendor). The molecular weight standards included phosphorylated (ovalbumin – 45.0 kDa; β-casein – 23.6 kDa) and non-phosphorylated (β-galactosidase – 116.2 kDa; BSA – 66.2 kDa; avidine – 18.0 kDa; lysozyme – 14.4 kDa) proteins.

that both fractions are highly purified (Fig. 1; note: empty lane 3 indicates that in m-TS no phosphate is detected, although lane 6 shows the presence of a single protein band, with subunits left unseparated. At the same time m-pTS shows the presence of phosphate, detected in lane 2. However, this modification concerns apparently only one subunit, causing differing electrophoretic mobilities of the two subunits, suggested by the two protein bands in lane 5). Moreover, it showed the phosphorylated fraction, or at least its prevailing part, to be modified on one subunit only (Fig. 1; *cf.* lanes 2 and 5; note: of the two protein bands stained in lane 5, corresponding to the two subunits (*cf.* ref. 16), only the upper one shows the presence of a phosphate group, as detected in lane 2, causing lower electrophoretic mobility of the phosphorylated subunit). Assuming the presence of a fraction of TS molecules phosphorylated on both subunits, it was too small to be detected. Alternatively, rare enzyme molecules that underwent phosphorylation in bacterial cells on both subunits could be lost in the process of MOAC, the loss also remaining undetected. The two TS fractions have been previously characterized by comparing their ^{31}P NMR spectra and found to contain unmodified and

Published on 17 February 2016. Downloaded by Politechnika Warszawska on 25/04/2016 09:51:58.

histidine-phosphorylated enzymes,[16] respectively. The latter was evidenced by the phosphorylated fraction spectrum containing a resonance at 2.14 ppm, belonging to inorganic phosphate, and two upfield shifted singlet peaks at −7.39 ppm and −9.87 ppm, with the singlet resonances in the negative spectrum region assigned to reflect *N*-phosphorylated histidine species (3-pHis and 1-pHis, respectively). The latter was confirmed by the acid-labile character of both resonances.[16] Different lines of evidence pointed to modification of His^{298} (affinity chromatography of a phosphate-containing peptide, followed by sequencing) and His^{33} (MS). In addition, by MS analysis phospho-Ser^{118} was determined.[16] It may not be excluded that the latter result, being in clear disagreement with the ^{31}P NMR spectra, is an artifact, as previously discussed.[16] Kinetic studies of both phosphorylated and non-phosphorylated TS fractions demonstrated the modification to be responsible for a 3-fold lower V_{max}^{app} (0.59 ± 0.05 μmol per min mg per protein *vs.* 1.64 ± 0.05 μmol per min mg per protein; $N = 5$), with unaltered K_m^{app} for either dUMP or meTHF.[16]

Inhibition of m-TS and m-pTS by FdUMP and N^4-OH-dCMP

Inhibition of mouse recombinant TS by FdUMP and N^4-OH-dCMP was examined with the use of the [5-^{3}H]dUMP tritium release activity assay. Each inhibitor, when preincubated with TS, in the presence of meTHF, caused time-dependent inactivation of the enzyme, consistent with the behavior as a slow-binding inhibitor.[25] While with the m-TS fraction treated with any of the two inhibitors, the inactivation rate did not change during preincubation, reflected by its linear dependence on time, with the m-pTS-catalyzed reaction, the same dependence was biphasic, reflecting apparently negative cooperativity of binding (Fig. 2 and Table 2). While with inactivation by FdUMP, the altered inactivation rate dependence on time resulted only in the later inactivation phase showing an almost 3-fold lower inhibition constant and over 10-fold lower inactivation rate constant, with N^4-OH-dCMP the effect of transition from the linear to biphasic inactivation profile was distinctly stronger. It amounted to a 5.5-fold increase of the inhibition constant, associated with an over 10-fold higher inactivation rate constant, followed by the later phase, characterized by the inhibition constant similar to that observed for m-TS, and inactivation rate constant 2.5-fold lower than that observed for m-TS, and over 10-fold lower than that observed for m-pTS during the earlier inactivation phase (Table 2).

With each of the two enzyme forms, both inhibitors form ternary complexes, reflected by gel shifts under conditions of non-denaturing electrophoresis (Fig. 3) and stable under conditions of SDS electrophoresis (Fig. 4). Comparison of the same gel stained for phosphate and later for protein allowed for monitoring of protein phosphorylation and the presence of a protein-bound nucleotide phosphate group. FdUMP is bound by m-TS only in the presence of meTHF (Fig. 3, *cf.* lanes 2 and 3), the complex moving faster than free enzyme under non-denaturing conditions (Fig. 3, lane 1). Apparently two forms of the complex, differing in mobility, are formed, containing presumably one (in the case of most TS molecules) or two inhibitor molecules bound per dimer. However, under denaturing conditions only the complex formed by one subunit remains stable, reflected by the protein pattern corresponding to free

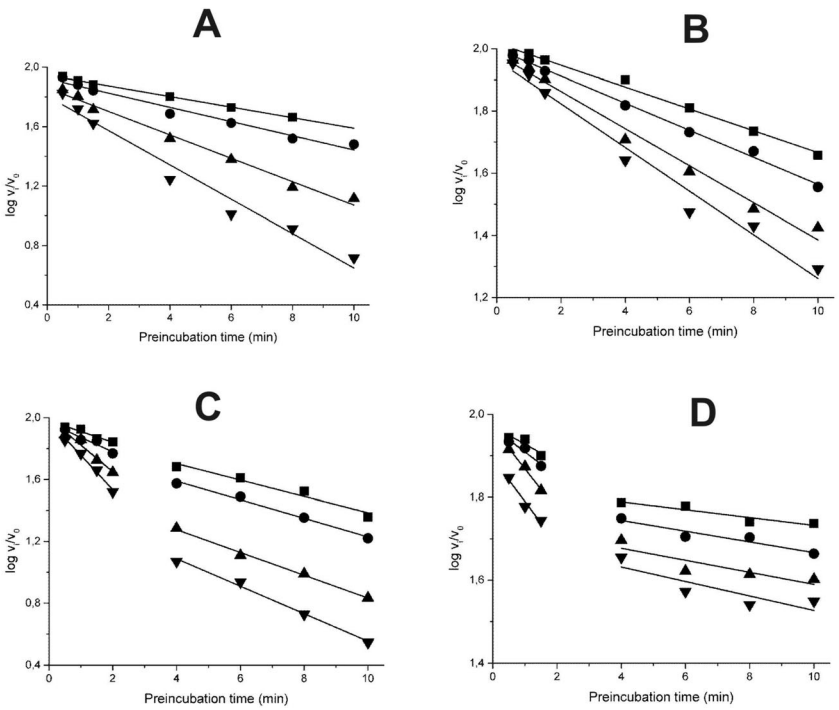

Fig. 2 Slow-binding inhibition of non-phosphorylated (panels A and B) and phosphorylated (panels C and D) fractions of mouse recombinant thymidylate synthase by FdUMP (panel A and C) and N^4-OH-dCMP (panels B and D). FdUMP concentrations were 9.14 nM (■), 12.8 nM (●), 21.3 nM (▲) and 32.0 nM (▼), and N^4-OH-dCMP concentrations were 0.29 μM (■), 0.41 μM (●), 0.68 μM (▲) and 1.02 μM (▼).

 This journal is © The Royal Society of Chemistry 2016

Published on 17 February 2016. Downloaded by Politechnika Warszawska on 25/04/2016 09:51:58.

Table 2 Parameters for inactivation by FdUMP and N^4-OH-dCMP of the m-TS and m-pTS fractions of mouse recombinant thymidylate synthase. For the biphasic plots of log (remaining activity) *vs.* time (*cf.* ref. 24), suggesting different interactions of each inhibitor with the two binding sites on the TS molecule, inhibition constants and inactivation rate constants were calculated with the use of the apparent inactivation rate constants during the initial (0.0–1.5 min) and later (4–10 min) periods of preincubation with a given inhibitor at various concentrations. The corresponding inhibition constants and inactivation rate constants are then K_i' and k_2' and K_i'' and k_2'', respectively

Enzyme protein	K_i' (nM)	K_i'' (nM)	k_2' (min^{-1})	k_2'' (min^{-1})
FdUMP				
m-TS[a]	4.8 ± 0.1 (3)		0.89 ± 0.13 (3)	
m-pTS	4.1 ± 1.1 (3)	0.32 ± 0.06 (3)	1.05 ± 0.15 (3)	0.087 ± 0.032 (3)
N^4-OH-dCMP				
m-TS[a]	14.3 ± 0.4 nM (3)		0.07 ± 0.01 (3)	
m-pTS[a]	77 ± 11.5 nM (3)	12.7 ± 1.1 (3)	0.41 ± 0.04 (3)	0.029 ± 0.008 (3)

[a] The inactivation rate did not change during the entire time of preincubation of the enzyme with the inhibitor; results are presented as means ± SEM, followed by the number of separate experiments in parentheses.

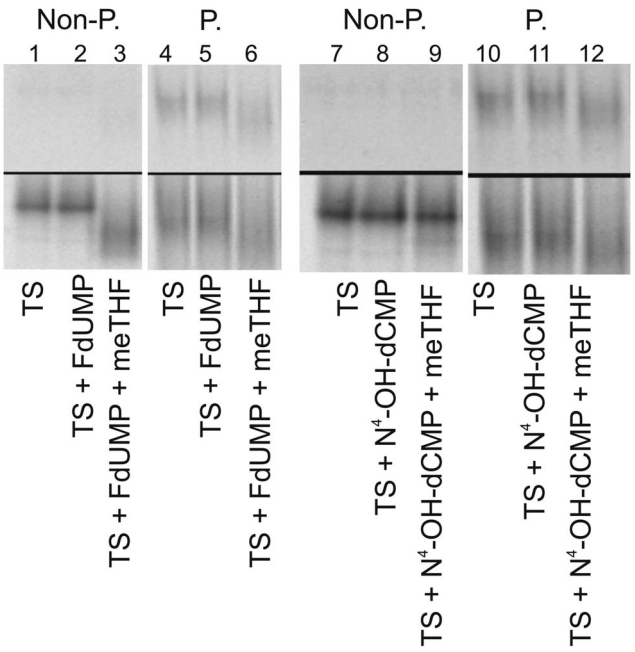

Fig. 3 Ternary complex formation by m-TS and m-pTS fractions with FdUMP and N^4-OH-dCMP in the presence of meTHF, monitored by non-denaturing-PAGE, with gels analyzed for phosphoprotein (upper part)/protein (bottom part); *cf.* Fig. 1 legend.

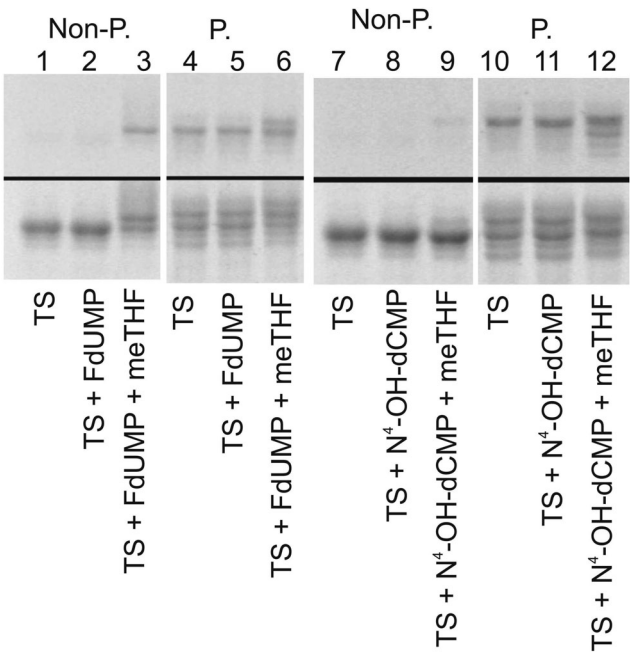

Fig. 4 Ternary complex formation by m-TS and m-pTS fractions with FdUMP and N^4-OH-dCMP in the presence of meTHF, monitored by SDS-PAGE, with gels analyzed for phosphoprotein (upper part)/protein (bottom part); *cf.* Fig. 1 legend.

enzyme separated into two bands, with only one of them (the slower) showing the presence of phosphate (Fig. 4, lane 3). With the phosphorylated enzyme form the picture is less sharp, presumably due to protein molecules being not uniformly phosphorylated, as suggested by MS results,[16] therefore showing small differences in mobilities. Nevertheless the shift of the ternary m-pTS–FdUMP–meTHF complex may be seen (Fig. 4, lane 6). Also with m-pTS only the complex formed by one subunit, the non-phosphorylated one, appears stable under denaturing conditions (Fig. 4, lane 6).

N^4-OH-dCMP appears to bind weaker to m-TS than m-pTS, causing only a small fraction of the mTS protein to shift under non-denaturing conditions and in the presence of meTHF with the complex presumably formed with one enzyme subunit (Fig. 4, lane 9) and remaining stable under denaturing conditions (Fig. 4, lane 9). The corresponding effects were definitely stronger with m-pTS (Fig. 3, lane 12 and Fig. 4, lane 12). Similar to FdUMP, N^4-OH-dCMP, in the presence of meTHF, bound only to the non-phosphorylated subunit (Fig. 4, lane 12).

Interestingly, the modification differing m-pTS from m-TS affected the time-dependent inactivation by each of the inhibitors studied (Fig. 2 and Table 2). The latter was of particular interest, as providing model evidence for a potential dependence on posttranslational modification of enzyme inhibition. It should be mentioned that previously studied TS nitration did not influence inhibition of the enzyme by FdUMP.[45] It should be noted that the difference between the parameters of inhibition by N^4-OH-dCMP of m-TS and m-pTS (Table 2) is reminiscent of the difference between the corresponding parameters of L1210p and L1210r inhibition by FdUMP (Table 1).

Published on 17 February 2016. Downloaded by Politechnika Warszawska on 25/04/2016 09:51:58.

Considering the influence of phosphorylation on the inactivation rate pattern (changing from linear to biphasic; Fig. 2), it appears to result from the asymmetry introduced by phosphorylation of only one subunit, at least in most molecules (Fig. 1). The latter seems to cause asymmetric binding of each inhibitor studied, reflected by the stability under denaturing conditions of complexes m-pTS–FdUMP–meTHF and m-pTS–N^4-OH-dCMP–meTHF, being formed only with the non-phosphorylated subunit (Fig. 4, lanes 6 and 12). Importantly, a consequence of TS being a half-the-sites reactive enzyme is that catalytic complex formation on one monomer renders the other monomer inactive,[35–37] with respect to both ligand binding and catalysis. Thus more frequent (if not exclusive) phosphorylation of one subunit appears to influence the latter mechanism by introducing subunit asymmetry and causing differing ligand binding and reactivity.

With respect to such a possibility, it is worth noting the results of MD simulations (based on the crystal structure 1I00), considering the dimeric structure of the human TS–dUMP–Tomudex complex, with antifolate replaced by the tetrahydrofolate (THF) molecule.[16] An interesting effect was noted on the binding behavior of ligands by phosphorylation at His^{304}, homologous to His^{298} in mTS (both found to undergo phosphorylation). With both active sites occupied by ligands, the alignment between the dUMP pyrimidine ring and THF pterin was dependent on whether phosphorylation concerned one or both subunits, in the former case being substantially disturbed in both subunits, whereas in the latter being much more disturbed on subunit A than B, where both ligands were more or less "in place", *i.e.* aligned parallel to each other (Fig. 5). Interestingly, no disturbance was apparent with only a single active site of the dimeric enzyme being occupied by the ligands.[16] It should be added that the above mentioned influence of His^{304} phosphorylation is a long-distance effect, as the distances between the centroids of the histidine imidazole and dUMP pyrimidine rings are: 23.3 Å and 25.2 Å in non-phosphorylated subunits A and B, respectively.

TS inhibition by FdUMP and N^4-OH-dCMP involves different molecular mechanisms. The former inhibitor forms with the enzyme and meTHF, in a reaction similar to that involving dUMP, a ternary covalently bound complex, with FdUMP C6 and C5 bound to the enzyme's catalytic Cys and meTHF methylene group, respectively.[46] The complex is stable, *i.e.* irreversibly bound, only under denaturing conditions. At this step the reaction stops, as the C(5) fluorine fails to dissociate (due to the strength of the C–F bond), as it happens with C(5) hydrogen in dUMP, resulting in a slowly reversible enzyme inactivation.[5] In contrast, the latter inhibitor appears to participate as a suicide substrate in an abortive enzyme-catalyzed reaction. Based on the crystal structure of a complex formed with the enzyme in the presence of N^4-OH-dCMP and meTHF (PDB ID: 4EZ8), the reaction appears to involve one-carbon group transfer to a hitherto unknown site, accompanied by THF oxidation to DHF and associated N^4-OH-dCMP pyrimidine C(5) reduction, leading to a covalently bound enzyme–inhibitor complex.[47] Stability, *i.e.* irreversible binding, of the latter complex was confirmed under denaturing conditions (Fig. 4, lane 12), as previously suggested for bacterial TS.[33]

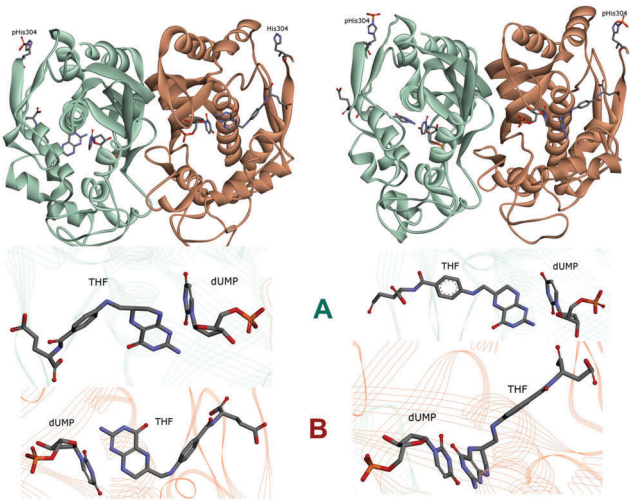

Fig. 5 Ribbon representation of the human TS–dUMP–THF complex structure, containing ligands in both active sites, with phosphorylated His^{304} residue (pHis) either in one (left) or both of the two subunits (right). Subunits are marked A (greenish blue) and B (brown). Below each of the two structures, enlarged fragments of active sites formed mainly by either subunit A or B, presenting the alignment between dUMP and THF. The distances between the centroids of the histidine imidazole and dUMP pyrimidine rings in subunits A and B are 23.7 Å and 25.4 Å (with $pHis^{304}$ on both subunits) or 24.0 Å and 23.4 Å (with $pHis^{304}$ only on subunit A), respectively. Based on MD simulations presented previously.[16]

Dependence of m-TS- and m-pTS inhibition by N^4-OH-dCMP on $[Mg^{2+}]$

Dependence on $[Mg^{2+}]$ for the inhibition by N^4-OH-dCMP of m-TS- and m-pTS-catalyzed reactions differed significantly. While with m-TS the degree of inhibition, defined as $(v_0 - v_i)/v_0$ (with v_i and v_0 being the initial rates determined in the presence and in the absence of the inhibitor, respectively), was only modestly dependent on $[Mg^{2+}]$, with m-pTS the dependence was biphasic, with the strongest inhibition observed at a concentration of ~40 mM (Fig. 6).

In view of the above presented hypothetical mechanism of TS inactivation by N^4-OH-dCMP, it should depend on the hydride transfer step of the TS-catalyzed reaction, causing THF oxidation (*cf.* ref. 5), and this step of bacterial TS-catalyzed reaction was recently found to be influenced by Mg^{2+} ions.[48,49] Interestingly, only inhibition of m-pTS by N^4-OH-dCMP was found strongly dependent on Mg^{2+} concentration, with the highest degree of inhibition at 40 mM Mg^{2+}, the concentration demonstrated previously to influence also mouse TS activity.[50] As this Mg^{2+} concentration is about one order of magnitude higher than those found in cells,[51] even considering the known uncertainty of cellular $[Mg^{2+}]$ measurements,[52] the effect may be without physiological relevance. However, of note is consistency with which previously studied endogenous enzyme forms, purified from different mouse tumour cells,[10,50] as well as the phosphorylated fraction of recombinant mouse enzyme studied here (Fig. 6), were sensitive only to Mg^{2+} at a certain range of concentrations (30–40 mM). Moreover, not only endogenous TS activation/inhibition,[10,50] but also an increase of the phosphorylated

 This journal is © The Royal Society of Chemistry 2016

Published on 17 February 2016. Downloaded by Politechnika Warszawska on 25/04/2016 09:51:58.

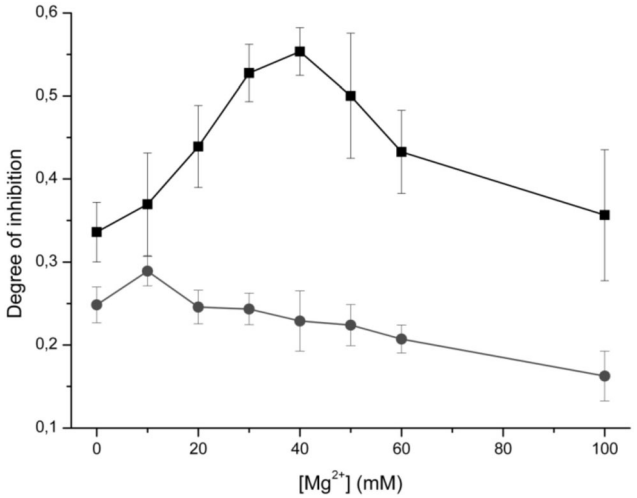

Fig. 6 Dependence on $[Mg^{2+}]$ for the degree of inhibition by 4 μM N^4-OH-dCMP of phosphorylated (■) and non-phosphorylated (●) mTS fractions. The enzyme reaction was run at 37 °C, with or without the inhibitor, in the presence of 0.625 mM (6*RS*)-meTHF, 54 μM [5-^{3}H]dUMP and various concentrations of $MgCl_2$, under conditions of a previously described enzyme activity assay.[50] Activity was determined by measurement of tritium release following 7 min incubation.[50] Compared values are degrees of inhibition, calculated as $(v_0 - v_i)/v_0$ (v_i and v_0 are the initial rates of the reaction running in the presence and in the absence of the inhibitor, respectively).

enzyme inhibition degree (Fig. 6), plotted as a function of $[Mg^{2+}]$, resulted in a bell-shaped curve, also observed with effects of the cation on other enzymes.[51,52]

Conclusions

With TSs of the same specific origin, differing slow-binding inhibition patterns, including biphasic or linear dependence of the inactivation rate on time, may result from varying post-translational modification statuses of the enzyme proteins, *e.g.* phosphorylated or non-phosphorylated. This may cause altered inhibition parameters, leading potentially to diminished TS sensitivity to inhibition and drug resistance. Further studies are needed to test the potential influence of other posttranslational modifications and their combinations.

Abbreviations

FdUrd	5-Fluoro-dUrd
FdUMP	5-Fluoro-dUMP
TS	Thymidylate synthase
meTHF	$N^{5,10}$-Methylenetetrahydrofolate
MOAC	Metal oxide/hydroxide affinity chromatography
m-pTS	Phosphorylated, MOAC-separated from the corresponding non-phosphorylated TS fraction of mouse enzyme recombinant protein
m-TS	Non-phosphorylated, MOAC-separated from the corresponding phosphorylated TS fraction of mouse enzyme recombinant protein
pHis	Phosphorylated His residue.

Acknowledgements

Supported by the National Science Centre (grant no. 2011/01/B/NZ6/01781).

References

1 A. Avallone, E. Di Gennaro, L. Silvestro, V. R. Iaffaioli and A. Budillon, Targeting thymidylate synthase in colorectal cancer: critical re-evaluation and emerging therapeutic role of raltitrexed, *Expert Opin. Drug Saf.*, 2014, **13**, 113–129.
2 F. G. Berger and S. H. Berger, Thymidylate synthase as a chemotherapeutic drug target: Where are we after fifty years? *Cancer Biol. Ther.*, 2006, **5**, 1238–1241.
3 P. M. Wilson, P. V. Danenberg, P. G. Johnston, H.-J. Lenz and R. D. Ladner, Standing the test of time: targeting thymidylate biosynthesis in cancer therapy, *Nat. Rev. Clin. Oncol.*, 2014, **11**, 282–298.
4 L. Taddia, D. D'Arca, S. Ferrari, C. Marraccini, L. Severi, G. Ponterini, Y. G. Assaraf, G. Marverti and M. P. Costi, Inside the biochemical pathways of thymidylate synthase perturbed by anticancer drugs: Novel strategies to overcome cancer chemoresistance, *Drug Resist. Updates*, 2015, **23**, 20–54.
5 C. W. Carreras and D. V. Santi, The catalytic mechanism and structure of thymidylate synthase, *Annu. Rev. Biochem.*, 1995, **64**, 721–762.
6 A. R. Waldorf and A. Polak, Mechanisms of Action of 5-Fluorocytosine, *Antimicrob. Agents Chemother.*, 1983, **23**, 79–85.
7 A. Vermes, H.-J. Guchelaar and J. Dankert, Flucytosine: a review of its pharmacology, clinical indications, pharmacokinetics, toxicity and drug interactions, *J. Antimicrob. Chemother.*, 2000, **46**, 171–179.
8 N. Suzuki, F. Nakagawa, M. Nukatsuka and M. Fukushima, Trifluorothymidine exhibits potent antitumor activity *via* the induction of DNA double-strand breaks, *Exp. Ther. Med.*, 2011, **2**, 393–397.
9 C. Heidelberger, G. Kaldor, K. L. Mukherjee and P. B. Danneberg, Studies on fluorinated pyrimidines. XI. *In vitro* studies on tumor resistance, *Cancer Res.*, 1960, **20**, 903–909.
10 M. M. Jastreboff, B. Kedzierska and W. Rode, Altered thymidylate synthetase in 5-fluorodeoxyuridine-resistant Ehrlich ascites carcinoma cells, *Biochem. Pharmacol.*, 1983, **32**, 2259–2267.
11 A. R. Bapat, C. Zarow and P. V. Danenberg, Human leukemic cells resistant to 5-fluoro-2′-deoxyuridine contain a thymidylate synthetase with lower affinity for nucleotides, *J. Biol. Chem.*, 1983, **258**, 4130–4136.
12 K. W. Barbour, D. K. Hoganson, S. H. Berger and F. G. Berger, A naturally occurring tyrosine to histidine replacement at residue 33 of human thymidylate synthase confers resistance to 5-fluoro-2′-deoxyuridine in mammalian and bacterial cells, *Mol. Pharmacol.*, 1992, **42**, 242–248.
13 C. T. Hughey, K. W. Barbour, F. G. Berger and S. H Berger, Functional effects of a naturally occurring amino acid

Published on 17 February 2016. Downloaded by Politechnika Warszawska on 25/04/2016 09:51:58.

substitution in human thymidylate synthase, *Mol. Pharmacol.*, 1993, **44**, 316–323.
14 H. Kawate, D. M. Landis and L. A. Loeb, Distribution of mutations in human thymidylate synthase yielding resistance to 5-fluorodeoxyuridine, *J. Biol. Chem.*, 2002, **277**, 36304–36311.
15 J. Cieśla, T. Frączyk, Z. Zieliński, J. Sikora and W. Rode, Altered mouse leukemia L1210 thymidylate synthase, associated with cell resistance to 5-fluoro-dUrd, is not mutated but rather reflects posttranslational modification, *Acta Biochim. Pol.*, 2006, **53**, 189–198.
16 T. Frączyk, T. Ruman, P. Wilk, P. Palmowski, A. Rogowska-Wrzesinska, J. Cieśla, Z. Zieliński, J. Nizioł, A. Jarmuła, P. Maj, B. Gołos, P. Wińska, S. Ostafil, E. Wałajtys-Rode, D. Shugar and W. Rode, Properties of phosphorylated thymidylate synthase, *Biochim. Biophys. Acta, Proteins Proteomics*, 2015, **1854**, 1922–1934.
17 D. Horn and M. T. Duraisingh, Antiparasitic Chemotherapy: From Genomes to Mechanisms, *Annu. Rev. Pharmacol. Toxicol.*, 2014, **54**, 71–94.
18 C. Walsh, Molecular mechanisms that confer antibacterial drug resistance, *Nature*, 2000, **406**, 775–781.
19 D. D. Richman, Antiviral drug resistance, *Antiviral Res.*, 2006, **71**, 117–121.
20 L. Strasfeld and S. Chou, Antiviral Drug Resistance: Mechanisms and Clinical Implications, *Infect. Dis. Clin. North Am.*, 2010, **24**, 413–437.
21 D. S. Perlin, E. Shor and Y. Zhao, Update on Antifungal Drug Resistance, *Curr. Clin. Microbiol. Rep.*, 2015, **2**, 84–95.
22 C. Holohan, S. Van Schaeybroeck, D. B Longley and P. G. Johnston, Cancer drug resistance: an evolving paradigm, *Nat. Rev. Cancer*, 2013, **13**, 714–726.
23 H. Zahreddine and K. L. Borden, Mechanisms and insights into drug resistance in cancer, *Front. Pharmacol.*, 2013, **4**, 28.
24 W. Rode, Z. Zieliński, J. M. Dzik, T. Kulikowski, M. Bretner, B. Kierdaszuk, J. Cieśla and D. Shugar, Mechanism of inhibition of mammalian tumour and other thymidylate synthases by N^4-hydroxy-dCMP, N^4-hydroxy-5-fluoro-dCMP and related analogues, *Biochemistry*, 1990, **19**, 10835–10842.
25 J. F. Morrison, The slow-binding and slow, tight-binding inhibition of enzyme-catalysed reactions, *Trends Biochem. Sci.*, 1982, **7**, 102–105.
26 W. Rode, J. Cieśla, Z. Zieliński and B. Kędzierska, Purification and properties of mouse thymus thymidylate synthase. Comparison of the enzyme from mammalian normal and tumour tissues, *Int. J. Biochem.*, 1986, **18**, 361–368.
27 W. Rode, T. Kulikowski, B. Kędzierska and D. Shugar, Studies on the interaction with thymidylate synthase of analogues of 2′-deoxyuridine-5′-phosphate and 5-fluoro-2′-deoxyuridine-5′-phosphate with modified phosphate groups, *Biochem. Pharmacol.*, 1987, **36**, 203–210.
28 W. Rode, M. Dąbrowska, Z. Zieliński, B. Gołos, M. Wranicz, K. Felczak and T. Kulikowski, *Trichinella spiralis* and *Trichinella pseudospiralis*: developmental patterns of enzymes involved in thymidylate biosynthesis and pyrimidine salvage, *Parasitology*, 2000, **120**, 593–600.
29 J. M. Dzik, T. Kulikowski, Z. Zieliński, J. Cieśla, W. Rode and D. Shugar, Interaction of 5-fluoro-4-thio-2′-deoxyuridine 5′-phosphate with mammalian tumour thymidylate synthase: role of the pyrimidine N(3)-H dissociation, *Biochem. Biophys. Res. Commun.*, 1987, **149**, 1200–1207.
30 J. M. Dzik, Z. Zieliński, J. Cieśla, M. Bretner, T. Kulikowski, D. Shugar, J. R. Bertino and W. Rode, Interaction of 2-thio-5-fluoro-dUMP and 4-thio-5-fluoro-dUMP with mammalian normal and tumour, and helminthic, thymidylate synthases: influence of C(4)-substituents on specificity for enzyme inactivation, *Biochem. Biophys. Res. Commun.*, 1993, **195**, 1301–1308.
31 M. Dąbrowska, Z. Zieliński, M. Wranicz, R. Michalski, K. Pawełczak and W. Rode, *Trichinella spiralis* thymidylate synthase: developmental pattern, isolation, molecular properties and inhibition by substrate and cofactor analogues, *Biochem. Biophys. Res. Commun.*, 1996, **228**, 440–445.
32 P. Wińska, B. Gołos, J. Cieśla, Z. Zieliński, T. Frączyk, E. Wałajtys-Rode and W. Rode, Developmental arrest in *C. elegans* dauer larvae leaves high expression of enzymes involved in thymidylate biosynthesis, similar to that found in *Trichinella* muscle larvae, *Parasitology*, 2005, **131**, 247–254.
33 S. Goldstein, A. L. Pogolotti, Jr., E. P. Garvey and D. V. Santi, Interaction of N^4-hydroxy-2′-deoxycytidilic acid with thymidylate synthetase, *J. Med. Chem.*, 1984, **27**, 1259–1262.
34 R. T. Reilly, K. W. Barbour, R. B. Dunlap and F. G. Berger, Biphasic binding of 5-fluoro-2′-deoxyuridylate to human thymidylate synthase, *Mol. Pharmacol.*, 1995, **48**, 72–79.
35 A. C. Anderson, R. H. O'Neil, W. L. DeLano and R. M. Stroud, The structural mechanism for half-the-sites reactivity in an enzyme, thymidylate synthase, involves a relay of changes between subunits, *Biochemistry*, 1999, **38**, 13829–13836.
36 R. L. Saxl, L. M. Changchien, L. W. Hardy and F. Maley, Parameters affecting the restoration of activity to inactive mutants of thymidylate synthase *via* subunit exchange: further evidence that thymidylate synthase is a half-of-the-sites activity enzyme, *Biochemistry*, 2001, **40**, 5275–5282.
37 M. Świniarska, A. Leś, W. Rode, J. Cieśla, C. Millán-Pacheco, I. O. Blake and N. Pastor, Segmental Motions of Rat Thymidylate Synthase Leading to Half-the-Sites Behaviour, *Biopolymers*, 2010, **93**, 549–559.
38 P. J. Sapienza, B. T. Falk and A. L Lee, Bacterial thymidylate synthase binds two molecules of substrate and cofactor without cooperativity, *J. Am. Chem. Soc.*, 2015, **137**, 14260–14263.
39 J. Cieśla, B. Gołos, E. Wałajtys-Rode, E. Jagielska, A. Płucienniczak and W. Rode, The effect of Arg209 to Lys mutation in mouse thymidylate synthase, *Acta Biochim. Pol.*, 2002, **49**, 651–658.
40 A. Wahba and M. Friedkin, The Enzymatic Synthesis of Thymidylate, *J. Biol. Chem.*, 1962, **237**, 3794–3801.
41 F. Wolschin, S. Wienkoop and W. Weckwerth, Enrichment of phosphorylated proteins and peptides from complex mixtures using metal oxide/hydroxide affinity chromatography (MOAC), *Proteomics*, 2005, **5**, 4389–4397.

 This journal is © The Royal Society of Chemistry 2016

Published on 17 February 2016. Downloaded by Politechnika Warszawska on 25/04/2016 09:51:58.

42 U. K. Laemmli, Cleavage of structural proteins during the assembly of the head of bacteriophage T4, *Nature*, 1970, **227**, 680–685.
43 J. M. Fujitaki and R. A. Smith, Techniques in the detection and characterization of phosphoramidate-containing proteins, *Methods Enzymol.*, 1984, **107**, 23–36.
44 C. B. Brouillette, C. T.-C. Chang and M. P. Mertes, 5-(α-Bromoacetyl)-2′-deoxyuridine 5′-phosphate: an affinity label for thymidylate synthetase, *J. Med. Chem.*, 1979, **22**, 1541–1544.
45 E. Dąbrowska-Maś, T. Frączyk, T. Ruman, K. Radziszewska, P. Wilk, J. Cieśla, Z. Zieliński, A. Jurkiewicz, B. Gołos, P. Wińska, E. Wałajtys-Rode, A. Leś, J. Nizioł, A. Jarmuła, P. Stefanowicz, Z. Szewczuk and W. Rode, Tyrosine nitration affects thymidylate synthase properties, *Org. Biomol. Chem.*, 2012, **10**, 323–331.
46 R. A. Byrd, W. H. Dawson, P. D. Ellis and R. B. Dunlap, Elucidation of the detailed Structures of the Native and Denatured Ternary Complexes of Thymidylate Synthetase *via* ^{19}F NMR, *J. Am. Chem. Soc.*, 1978, **100**, 7478–7486.
47 A. Dowierciał, A. Jarmuła, P. Wilk, W. Rypniewski, B. Kierdaszuk and W. Rode, Crystal structures of complexes of mouse thymidylate synthase crystallized with N^4-OH-dCMP alone or in the presence of $N^{5,10}$-methylenetetrahydrofolate, *Pteridines*, 2013, **24**, 93–98.
48 Z. Wang, P. J. Sapienza, T. Abeysinghe and C. Luzu, Mg^{2+} binds to the surface of thymidylate synthase and affects hydride transfer at the interior active site, *J. Am. Chem. Soc.*, 2013, **135**, 7583–7592.
49 P. Singh, T. Abeysinghe and A. Kohen, Linking Protein Motion to Enzyme Catalysis, *Molecules*, 2015, **20**, 1192–1209.
50 W. Rode and M. M. Jastreboff, Effects of Mg^{2+} and adenine nucleotides on thymidylate synthetase from different mouse tumors, *Mol. Cell. Biochem.*, 1984, **60**, 73–76.
51 T. Günther, Concentration, compartmentation and metabolic function of intracellular free Mg^{2+}, *Magnesium Res.*, 2006, **19**, 225–236.
52 H. Ebel and T. Günther, Magnesium metabolism: a review, *J. Clin. Chem. Clin. Biochem.*, 1980, **18**, 257–270.